



HAL
open science

The ionospheric scintillation phenomenon

Aurelien Galmiche, Sébastien Trilles, Sébastien Rougerie, Vincent Fabbro,
Laurent Féral, Julie Lapie, Louis Bakienon

► **To cite this version:**

Aurelien Galmiche, Sébastien Trilles, Sébastien Rougerie, Vincent Fabbro, Laurent Féral, et al.. The ionospheric scintillation phenomenon. Inside GNSS, 2022, Ionospheric scintillation in West Africa, pp.44-53. hal-03865661

HAL Id: hal-03865661

<https://hal.science/hal-03865661v1>

Submitted on 4 Jan 2023

HAL is a multi-disciplinary open access archive for the deposit and dissemination of scientific research documents, whether they are published or not. The documents may come from teaching and research institutions in France or abroad, or from public or private research centers.

L'archive ouverte pluridisciplinaire **HAL**, est destinée au dépôt et à la diffusion de documents scientifiques de niveau recherche, publiés ou non, émanant des établissements d'enseignement et de recherche français ou étrangers, des laboratoires publics ou privés.

THE IONOSPHERIC SCINTILLATION PHENOMENON

*Aurélien Galmiche⁽¹⁾, Sébastien Trilles⁽¹⁾, Sébastien Rougerie⁽¹⁾, Vincent Fabbro⁽²⁾, Laurent Féral⁽³⁾,
Julien Lapie⁽⁴⁾, Louis Bakienon⁽⁴⁾*

(1) : Thales Alenia Space, (2) : ONERA/DEMR, (3) : Laboratoire d'Aérodynamique, UMR 5560, (4) :
ASECNA

A. ABSTRACT

The Satellite Based Augmentation System ASECNA for Africa & Indian Ocean (A-SBAS), led by the Agency for Air Navigation Safety in Africa and Madagascar (ASECNA), an international organization of 18 Member States in charge of air navigation services provision in an 16 millions squared km, is under development in view of services declaration in the next years. A-SBAS is recognized by the International Civil Aviation Organisation (ICAO) as the part of the Global Navigation Satellite Systems (GNSS) infrastructure. It is designed to deliver a safe positioning accuracy by augmenting GPS satellite navigation constellation with differential corrections and integrity data, in order to enable advanced navigation operations down to precision approaches in all runways ends in Africa. The core of the SBAS mission consists in decomposing all possible range error sources and distributing corrections and/or alerts to its users by means of geostationary satellites. The major range error source affecting the A-SBAS system performances is the ionosphere dynamic because the magnetic equator, as a main driver, crosses the West-ern African sector. This particular latitudinal situation is one of the factors leading to the apparition of the ionospheric scintillation at night and close to the equinoxes in this area.

The SAGAIE network of GNSS stations was therefore deployed in West-ern Africa in 2013 by CNES and ASECNA to assess the feasibility of an equatorial SBAS for ASECNA area by studying the phenomenon which has a strong negative influence on the GNSS signals – among others. This study of SAGAIE network's measurements therefore aims at analyzing the characteristics of the scintillation recorded by the five receivers covering the Sub-Saharan West-Africa, between the years 2013 and 2016. This period of time covers almost half a solar cycle, with which the scintillation has been highly varying. It is shown that scintillation has a temporal global pattern well marked in the five SAGAIE stations: an increase after local sunset, a peak between 8 and 11pm, and a decrease overnight. The amplitude of the phenomenon increases close to the equinoxes, where scintillation is at its maximum. However, variability in temporal occurrence or magnitude with longitude and latitude has also been observed in the different stations. Spatially, the well-known equatorial crests where the scintillation maximums occur are well observed through SAGAIE, north and south of the magnetic equator. The low elevation, increasing scintillation indices, has been shown to play a minor role in their characterization. Finally, the strong influence of the solar activity on equatorial scintillation was highlighted through the comparison of solar peak data versus data from a lower solar activity period.

Index Terms - propagation, scintillation, GNSS, ionosphere, SAGAIE, Africa, ASECNA A-SBAS.

1. INTRODUCTION

The ionospheric scintillation phenomenon is characterized by a strong fluctuation of the phase and amplitude of the radio wave received on Earth. It is due to small-scale irregularities of the electronic concentration of the plasma crossing the beam of the incident signal. Close to the magnetic equator for instance, scintillation has been linked with the equatorial anomaly [Rishbeth, 1997]. Waves with frequencies up to 12 GHz can be affected by ionospheric scintillation [ITU-R P531-14, 2019]. Therefore, scintillation is of great concern for applications with high service availability such as GNSS : in addition to increasing the noise and reducing the accuracy of the estimated position of a user, it can lead to cycle slips, and even to the loss of lock of the satellite-to-Earth link. The study of scintillation is hence needed to understand the features of the phenomenon, linked with the atmosphere and the Sun's physics. Mention is made of different behaviors depending on latitude and longitude of the observation. Literature lacks of global studies made on the African continent. However, Africa is the continent where civil aviation will experience the most important growth in the next 10 years. The emergence of satellite augmentation GNSS technologies, providing Safety-Of-Life aeronautic operations as they exist in North-America (WAAS), Europe (EGNOS), India (GAGAN) or Japan (MSAS) to assist the user needs to take into account this destructive phenomenon.

Among the different patterns followed by scintillation, different studies have shown a clear dependence of frequency and intensity of scintillation with the Sun's activity (that can be quantified by Sun Spot's Number) [Fejer, 1991]. The cycle of the Sun's activity n°24, which was rather weak compared to the cycles 22 and 23, had its activity peak between 2013 and 2014, and it is currently ending. The next solar cycle's maximum shall not happen before 2025 according to studies [Bhomik &

Ionospheric scintillation in West Africa

48 Nandy, 2018]. The SAGAIE stations that observed the Sub-Saharan West-African ionosphere from 2013 until present is hence
49 a powerful tool to study the ionospheric scintillation in the scope of a characterization of the phenomenon.

50 The detailed features of this network will be introduced in section 2 of this paper. Ionospheric index S_4 is well suited when
51 scintillation is to be studied at low latitude; section 3 will focus on the temporal study of the amplitude scintillation. Section 4
52 will study the spatial distribution of S_4 in the West-African sector. The link between scintillation and the solar cycle seen
53 through SAGAIE in Africa will be described in section 5.

54 55 **2. PRESENTATION OF THE SAGAIE DATABASE**

56
57 A network of GNSS stations deployed in the African equatorial region, and measuring the ionospheric scintillation is an
58 interesting way to measure the spatial and temporal dynamic of the ionospheric plasma. Indeed, the L-band is subject to the
59 ionosphere's variations while always crossing the medium. Therefore, the SAGAIE network seems perfectly adapted to analyze
60 the turbulent ionosphere in this special area of the world. SAGAIE is an acronym corresponding to Stations ASECNA GNSS
61 pour l'Analyse de l'Ionosphère Equatoriale, or in English, GNSS ASECNA Stations for the Analysis of the Equatorial
62 Ionosphere, where ASECNA stands for Agence pour la Sécurité de la Navigation Aérienne en Afrique et à Madagascar, or
63 Agency for the Air Navigation Safety in Africa and Madagascar. SAGAIE network is a cooperation between the French Space
64 Agency CNES and ASECNA, financed by CNES and hosted by ASECNA. It was operated and maintained by Thales Alenia
65 Space until 2021. It began its service in 2013. It will be further extended in the coming years and is operated by CNES since
66 2021. The accumulation of data since 2013 by SAGAIE enables a wide characterization of the ionospheric conditions observed
67 since the peak of solar cycle 24. The aim of this network is also to challenge the robustness of GNSS algorithms, especially the
68 ones embarked on aircrafts equipped with SBAS (Satellite-Based Augmentation System) technology [Secretan et al., 2014].
69 The SAGAIE network is composed of five stations in West-ern and Central Africa. The stations are located in Dakar (Senegal),
70 Ouagadougou (Burkina Faso), N'Djamena (Chad), Douala (Cameroon), and Lome (Togo). Their positions are shown in the
71 Figure 1.

72 ASECNA premises host the stations. The use of such quality facilities prevents power outage, and enables an internet link for
73 real-time ionospheric analysis. The stations' installation was preceded by a study phase which aimed to minimize the data
74 corruption by undesired propagation effects such as ground multipath. The five SAGAIE stations were compared to the IGS
75 sites (International GNSS Service) through a GPS bi-frequency signal quality check. The five stations were ranked among the
76 best IGS stations in the world in terms of multipath [Secretan et al., 2014].

77 Two kinds of receivers were used to collect the GNSS data of SAGAIE :

- 78 - A multi-frequency (whole L band), multi-constellation (GPS, GLONASS, Galileo, SBAS) scintillation monitor PolaRxS
79 Pro ISM manufactured by Septentrio
- 80 - A multi-frequency (L1, L5, L2), multi-constellation (GPS, GLONASS, Galileo, SBAS) GNSS receiver FlexPak 6
81 OEM628 manufactured by Novatel.

82 The stations of Dakar and Lome are equipped with both receivers and a "choke ring" Septentrio antenna, whereas the three
83 other stations are equipped only with the FlexPak 6 OEM628 Novatel receiver. Ouagadougou, Douala and N'Djamena receive
84 signal through a Novatel A703 antenna.
85

Ionospheric scintillation in West Africa

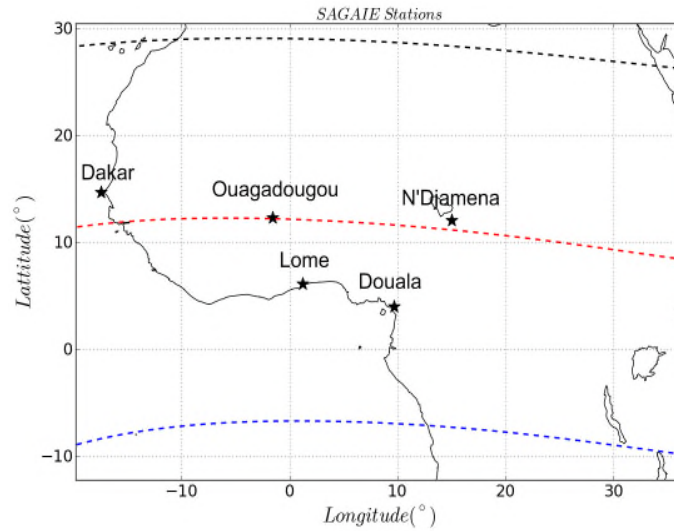


Figure 1 – Position of the five SAGAIE stations with the geomagnetic equator (in dotted red line), 20° north of the geomagnetic equator, and 20° south of the geomagnetic equator. All stations are contained within 10° of the geomagnetic equator.

The first observations made by the network show a strong link between the medium-to-strong scintillation events, and the satellites' elevation observed from the stations, the equinoxes period, the hour of the day [Secretan et al., 2014]. These observations are in line with previous results on the equatorial scintillation from the literature [Aarons, 1993][Moraes et al., 2017].

In this paper, ionospheric scintillation is studied through the amplitude scintillation index S_4 , which is obtained as described in [Van Dierendonck et al., 1993]:

$$S_4 = \sqrt{\frac{\langle C/N_0^2 \rangle - \langle C/N_0 \rangle^2}{\langle C/N_0 \rangle^2}}$$

Where symbol $\langle \rangle$ refers to the average operator, performed on one minute of data. The signal intensity is here supposed to be given by the signal to noise ratio C/N_0 [Van Dierendonck et al., 1993]. C/N_0 is here a vector, sampled at 1 Hz. It is obtained from the SAGAIE GNSS receivers through a Thales Alenia Space – designed processor. Since the average operator is performed on one minute, for each S_4 calculated using expression (1), 60 values of C/N_0 are used in a nominal case. If the link is temporarily unavailable, and 20 values of C/N_0 or less are processed, the S_4 index status is set to unavailable, so that it does not fool the measurements. An elevation mask of 30° is usually applied in such studies to avoid ground multipath [Mushini, 2012]. However, the favorable environment of the SAGAIE stations permitted to choose a 15° elevation mask without being troubled by multipath or other undesired propagation effects, as shown by measurement quality analysis performed by Thales Alenia Space algorithmic core [Foucault et al., 2018]. More line-of-sight can therefore be observed to characterize the medium. The period during which data were observed in this paper ranges from august 2013 to august 2016. As presented on the Figure 2, this period was chosen to cover the maximum and the decrease of the solar cycle 24. The Sun Spot Number is here used as a proxy for solar activity, [Bhomik & Nandy, 2018] in order to be able to observe a possible variability of scintillation over the intensity of the solar activity, as mentioned by [Fejer, 1991].

Ionospheric scintillation in West Africa

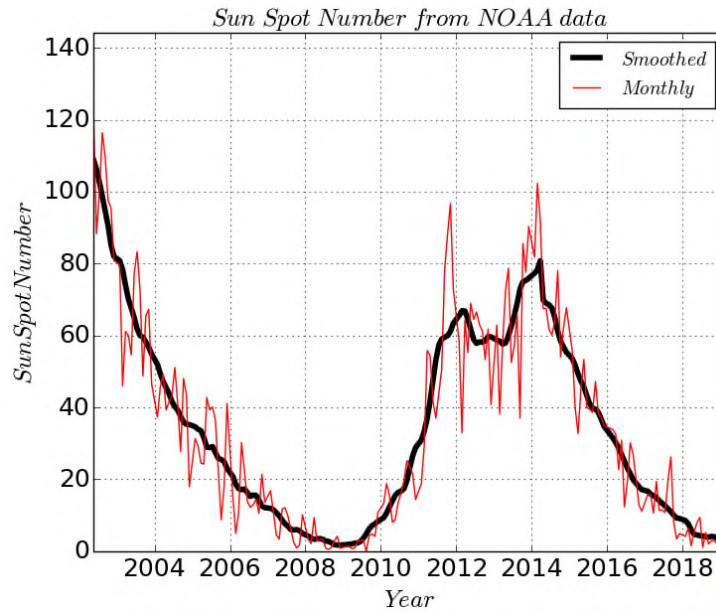


Figure 2 – Solar cycle Sun Spot Number observed between 2003 and December 2019, data from NOAA :
<https://www.swpc.noaa.gov>.

112
113
114

In total, more than 60 million S_4 values have been calculated over the time frame selected. The repartition of those values between the five stations is presented in the Table 1, as well as the number of S_4 above a threshold of 0.5. There is a good balance of the number of S_4 indices observed between the five stations ; this will permit interesting comparative studies, which are conducted in the next sections.

The number of $S_4 > 0.5$ is quite significant: between 14 thousand and 37 thousand depending on the stations ($S_4 > 0.5$ is characteristic of medium-to-strong scintillation events according to [Mushini, 2012] and [ITU-R P531-14, 2019]). This denotes a variable state of the ionosphere during the time of observation between steadiness and turbulence. Next sections will also focus on describing those variations.

123
124

Table 1 – Number of $S_4 > 0.5$ measured and total number of S_4 measured in the five SAGAIE stations.

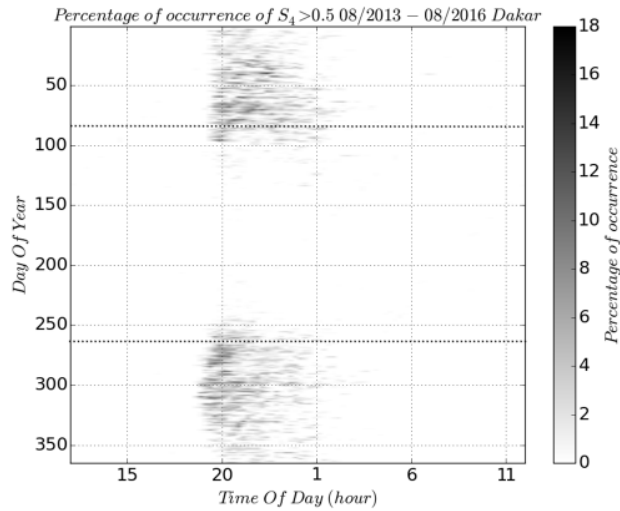
	DAK	OUA	LOM	NDJ	DOU
$N(S_4 > 0.5)$	26 042	19 428	28 938	14 164	37 294
$N(S_4)/1000$	12 540	12 158	12 201	11 891	11 889

125
126
127
128
129
130
131
132
133
134
135
136

3. TEMPORAL STUDY OF THE S_4 INDEX

The study of this section refers to the temporal variability of the S_4 index on the West-African Sub-Saharan region. From the Figure 3 to the Figure 7 are plotted in gray scale the percentage of occurrence for S_4 to be observed above the threshold 0.5, against the hour of the day in local time (x-axis) and the day of the year (y-axis) for the five SAGAIE stations. On the Figure 8, the same quantity is represented, but averaged on the five SAGAIE stations. The value of $S_4 > 0.5$ usually denotes a scintillation that can severely impact the GNSS systems [Rama Rao et al., 2006][Guo et al., 2019]. This study hence refers to medium-to-strong scintillation events.

Ionospheric scintillation in West Africa



137

138

139

Figure 3 – Percentage of occurrence of S_4 index measured over 0.5 as a function of the day of year and the local solar hour in Dakar, Senegal, between 08/2013 and 08/2016. The dotted lines show the equinoxes of spring and fall.

140

141

142

143

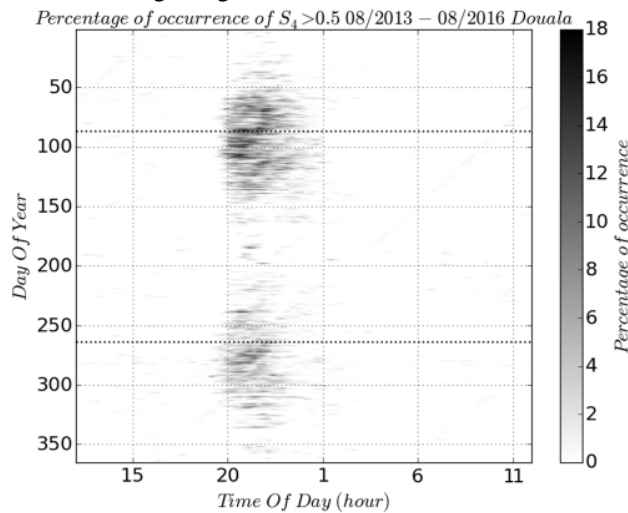
144

145

146

147

A global tendency is observed and common to all stations : ionospheric scintillation appears around 8pm solar time (i.e. 20h), and disappears around 1am, solar time (i.e. 1h). The peaks of scintillation occurrence are observed during or close to the equinoxes, in agreement with what was previously reported in the literature [Aarons, 1993][Moraes et al., 2017]. On the Figure 8 (an average calculation of the Figure 3 to the Figure 7), we remark that scintillation extracted from the SAGAIE measurements seems more frequent and more intense close to the spring equinox than close to the fall equinox. The dissymmetry between the two equinoxes is particularly well marked on the Figure 4 from Douala, and Figure 5 from Lome, and can be distinguished in Figure 6 in N'Djamena and Figure 7 from Ouagadougou.



148

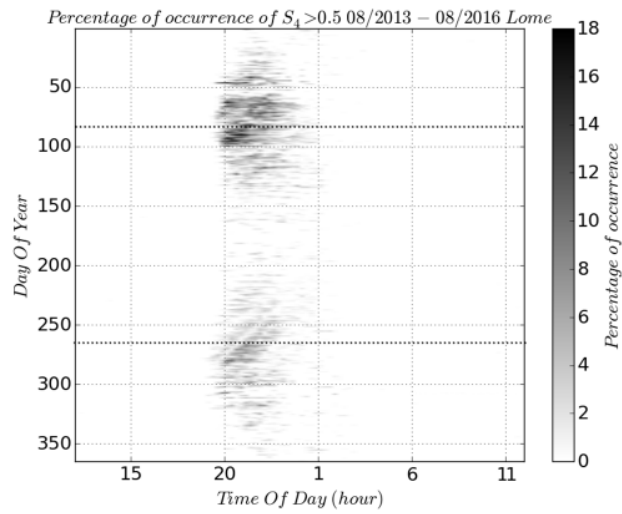
149

150

151

Figure 4 – Percentage of occurrence of S_4 index measured over 0.5 as a function of the day of year and the local solar hour in Douala, Cameroon, between 08/2013 and 08/2016. The dotted lines show the equinoxes of spring and fall.

Ionospheric scintillation in West Africa



152

153

154

155

Figure 5 – Percentage of occurrence of S_4 index measured over 0.5 as a function of the day of year and the local solar hour in Lome, Togo, between 08/2013 and 08/2016. The dotted lines show the equinoxes of spring and fall.

156

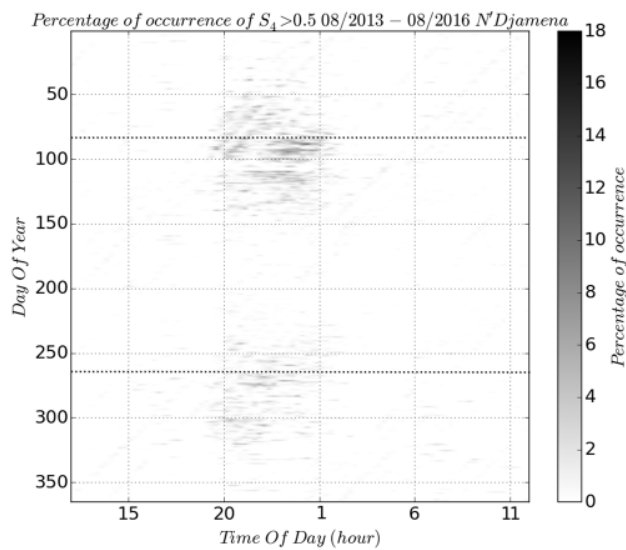
157

158

159

160

However, scintillation characteristics linked with the latitude and the longitude seem to differ for the five stations. In N'Djamena in Figure 6 and in Ouagadougou in Figure 7, ionospheric scintillation appears before 8pm and ends slightly after 1am, whereas in Lome in Figure 5, and in Douala in Figure 4, scintillation ends before 1 am. In Dakar in Figure 3, scintillation starts earlier, around 7pm, and ends after 1am, the phenomenon hence lasts globally longer than in the other stations.



161

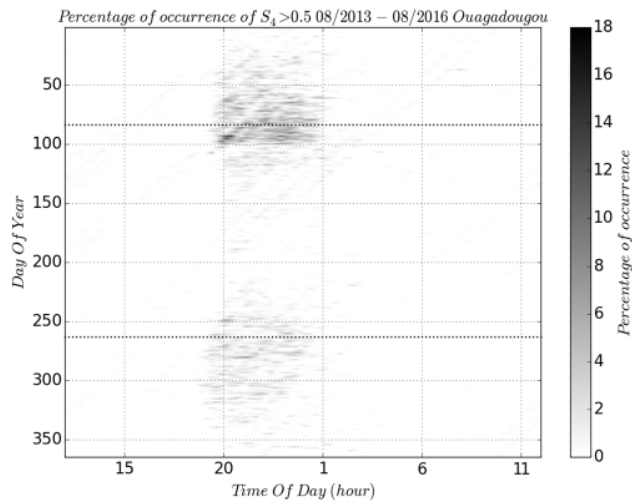
162

163

164

Figure 6 – Percentage of occurrence of S_4 index measured over 0.5 as a function of the day of year and the local solar hour in N'Djamena, Chad, between 08/2013 and 08/2016. The dotted lines mark the equinoxes of spring and fall.

Ionospheric scintillation in West Africa



165

166

167

168

169

Figure 7 – Percentage of occurrence of S_4 index measured over 0.5 as a function of the day of year and the local solar hour in Ouagadougou, Burkina Faso, between 08/2013 and 08/2016. The dotted lines show the equinoxes of spring and fall.

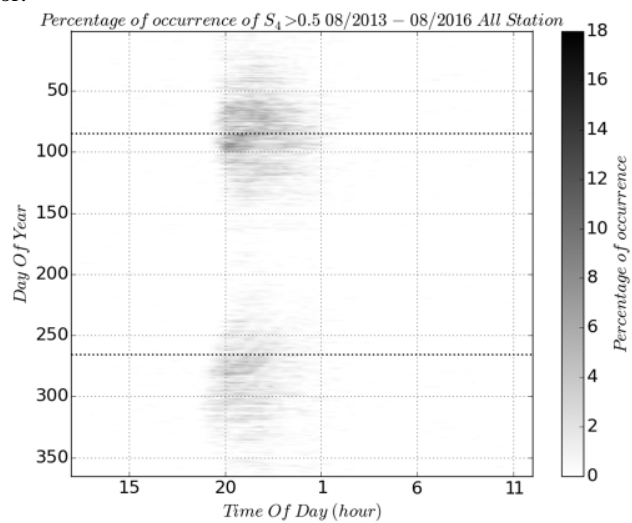
170

171

172

173

The phenomenon hence seems to last less in the two stations closer to the magnetic equator (Ouagadougou and N'Djamena), while the duration is maximum in Dakar. Ionospheric scintillation observed through SAGAIE therefore shows more frequent and intense amplitude scintillation from the stations close to the equatorial crests, between 5 and 15 degrees of latitude north and south of the magnetic equator.



174

175

176

177

Figure 8 – Percentage of occurrence of S_4 index measured over 0.5 as a function of the day of year and the local solar hour averaged in the five SAGAIE stations, between 08/2013 and 08/2016. The dotted lines show the equinoxes of spring and fall.

178

179

180

181

182

183

184

These conclusions can be partially retrieved through the analysis of the Table 1. The number of S_4 measured is similar for all stations (it is not exactly the same due to both the visibility of the satellites in the sky and the punctual loss of internet network resulting in minor data loss), the two stations of N'Djamena and Ouagadougou have less $S_4 > 0.5$ than other. It confirms the conclusions previously stated, showing that the scintillation in those places close to the magnetic equator is less intense than in Douala, where there are twice as many events for which $S_4 > 0.5$. The Figure 4 also shows percentage of occurrence of $S_4 > 0.5$ close to 20% during equinoxes, with a great duration in time, something neither observed in Ouagadougou nor in

Ionospheric scintillation in West Africa

185 N'Djamena. The number of scintillation events for which $S_4 > 0.5$ is also greater in Dakar and Lome than in N'Djamena and
186 Ouagadougou, showing a higher presence of medium-to-strong scintillation events in those places. Those are some hints of the
187 geographical characteristics of the equatorial scintillation, which are detailed in the next section (4).

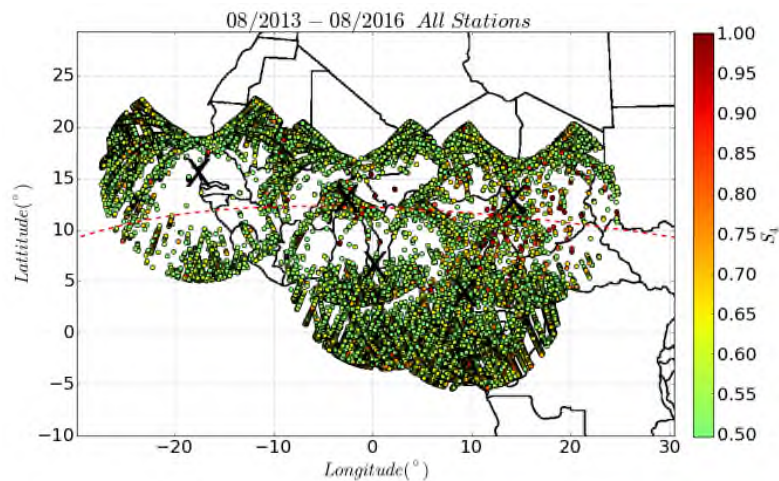
188 4. SPATIAL STUDY OF THE S_4 INDEX

189
190 The mean IPP (Ionospheric Pierce Point, calculated at a height of 400 km) of the events for which S_4 has been measured over
191 the thresholds 0.5 and 0.7 are shown on the Figure 9 and the Figure 10, respectively. The color of the point shows the measured
192 value of S_4 with respect to the adjacent color bar. The position of the geomagnetic equator is represented in dotted red line in
193 the two figures. The locations of the SAGAIE stations are highlighted by black crosses. More than 125 000 events are displayed
194 on the Figure 9, and 25 000 are displayed on the Figure 10, showing the significant number of medium-to-strong scintillation
195 events. Those two figures hence show the geographical positions of the places where medium-to-strong (threshold on S_4 of
196 0.5) and strong (threshold on S_4 of 0.7) ionospheric scintillation has been observed.

197 In the Figure 9, it is common to notice events for which $S_4 > 0.5$ close to the geomagnetic equator, even though most of the
198 events are north and south of this line. In the Figure 10, the vast majority of the events are located north and south of the
199 geomagnetic equator. The location of these strong scintillation events shows the presence of well-marked equatorial crests,
200 between the latitudes 15° and 20° (north crest), and between the latitude -5° and 5° (south crest). As it was remarked in section
201 3, the station of Douala contributes well to the observation of strong scintillation ; indeed, this station is the furthest away from
202 the geomagnetic equator, and the majority of the events for which $S_4 > 0.7$ has been observed from there.

203 These equatorial crests observations are in agreement with the common description of scintillation apparition, linked with the
204 phenomenon of equatorial fountains [Klobuchar, 1991] [Bllely & Alcaydé, 2007].

205



206

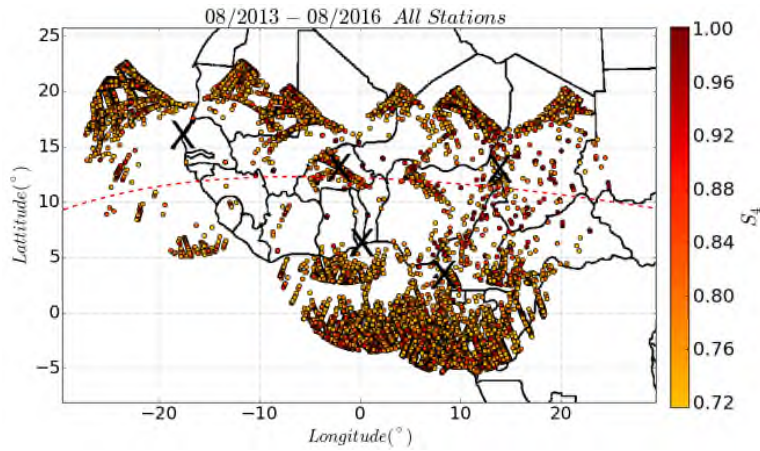
207 **Figure 9 – Mapping of the IPP of events for which $S_4 > 0.5$ observed between 08/2013 and 08/2016. The color of the**
208 **dot indicates the value of the S_4 measured. The geomagnetic equator is in red.**

209

210 Events of moderate-to-strong scintillation appear east and west of the SAGAIE stations such as Dakar, Ouagadougou and
211 N'Djamena in the Figure 9. Those places do not belong to the equatorial crests, and should therefore not be subject to strong
212 scintillation. However, it is known that S_4 index is inversely proportional to the elevation angle, as shown by [Rino, 1979] or
213 [Galiègue et al., 2016]. This effect then contributes to increase the S_4 indices at low elevations. However, a partial decorrelation
214 of the scintillation (particularly the S_4 index) and the elevation angle under which the signal is received can be seen. Indeed,
215 there are only a few strong scintillation events located east and west of the SAGAIE stations in the Figure 10, whereas many
216 events are seen north and south of the stations (i.e. located on the equatorial crests), though that are seen with the same elevation
217 than east and west events.

Ionospheric scintillation in West Africa

218

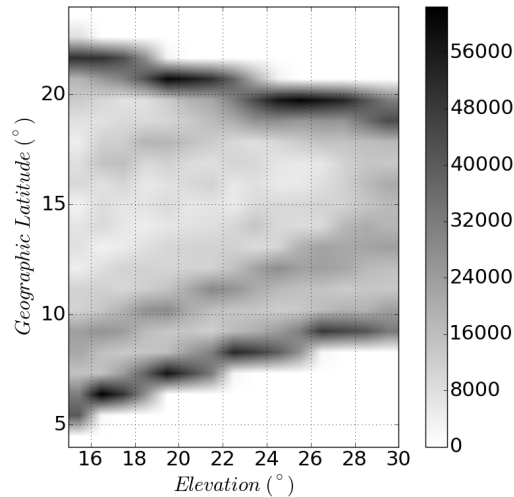


219

220

221

Figure 10 – Mapping of the IPP of events for which $S_4 > 0.7$ observed between 08/2013 and 08/2016. The color of the dot indicates the value of the S_4 measured. The geomagnetic equator is in red.



222

223

224

225

Figure 11 - Number of measurements from Dakar between 08/2013 and 08/2016 against the elevation under which they are seen (x-axis, in degrees) and against the latitude of their IPP (y-axis, in degrees). The number is indicated by the shade of grey, reported on the adjacent color bar.

226

227

228

229

230

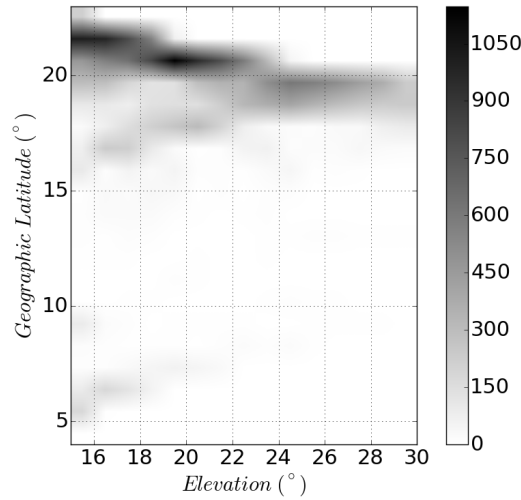
231

232

233

Focusing only on the Dakar station, the Figure 11 shows the number of S_4 measurements against their elevation seen from Dakar (x-axis) and the latitude of their IPP (y-axis), while the Figure 12 represents the same quantity, but only for events having $S_4 > 0.5$ respectively. Figure 12 clearly shows, between elevations 15 and 30°, more events at high latitudes (15 to 23° north) than at low latitude (below 10°N), whereas Figure 11 shows that the number of IPP in sight is approximately the same for low and high latitude under those elevations. The north equatorial crest is roughly located between 15 and 25° north in Dakar, whereas no crest is present between 5 and 15° north. This clearly shows a dependence of scintillation to the equatorial physics, and not only in the elevation.

234



235

236

237

238

Figure 12 - Number of events for which $S_4 > 0.5$ seen from Dakar between 08/2013 and 08/2016 against the elevation under which they are seen (x-axis, in degrees) and against the latitude of their IPP (y-axis, in degrees). The number is indicated by the shade of grey, reported on the adjacent color bar.

239

240

241

242

5. SCINTILLATION AND SOLAR CYCLE

243

244

245

Another major feature of the scintillation impacting both the geographical distribution and temporal occurrence of the event was observed through SAGAIE : this is the dependence of the scintillation with the solar cycle.

246

247

From the Figure 2, it is possible to notice that the highest peak of solar cycle 24 occurs at the beginning of the year 2014, while 2016 is a year counting a Sun Spot Number three times lower in average and is therefore a weaker year.

248

249

250

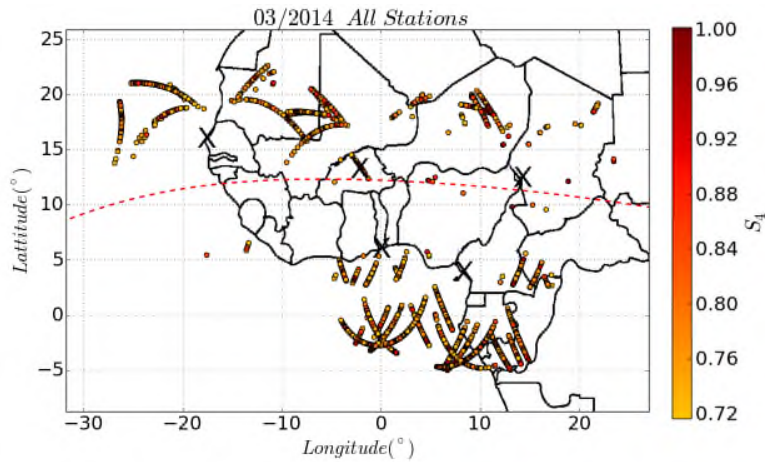
251

252

The mean IPP of the events for which S_4 has been measured over the thresholds 0.7 are shown on the Figure 13 for the month of March 2014 and on the Figure 14 for the month of March 2016. The color of the point shows the measured value of S_4 with respect to the adjacent colorbar. The position of the geomagnetic equator is represented in red dashed line. The locations of the SAGAIE stations are highlighted by black crosses. As shown in section 3, the month of March is a month of strong scintillation for the SAGAIE network.

Ionospheric scintillation in West Africa

253



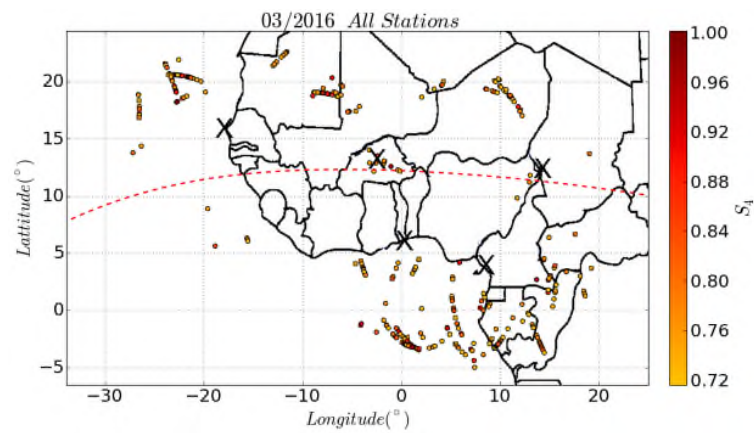
254

255

256

257

Figure 13 - Mapping of the IPP of events for which $S_4 > 0.7$ observed in March 2014. The geomagnetic equator is in red dashed line.



258

259

260

261

Figure 14 - Mapping of the IPP of events for which $S_4 > 0.7$ observed in March 2016. The geomagnetic equator is in dotted red line.

262

263

264

265

266

The conclusions of section 4 on the elevation and on the geographical position of the IPP can also be inferred from the Figure 13 and the Figure 14. Clearly, less strong scintillation events (i.e. $S_4 > 0.7$) were observed in March 2016 (337) than in March 2014 (2804); that is more than 13 time less events in March 2016 than in March 2014. Ionospheric scintillation, and in particular events apt to influence severely the GNSS signals clearly depend on the solar activity.

267

268

269

270

271

272

It is then useful recalling that the SAGAIE data started to be measured in 2013; the study of scintillation presented in this paper hence globally refers to a weak solar cycle (24) when it is compared to solar cycles 22 or 23 [Bhomik et al., 2018]. Therefore, the conclusions of the frequency and intensity of ionospheric scintillation events might be under-estimated compared to the two previous solar cycles. The levels of ionospheric scintillation observed could have been drastically increased if the data had been measured during solar cycle 22 for instance, which peak counted Sun Spot Numbers two times higher in average than the peak of solar cycle 24.

273

6. CONCLUSION AND FUTURE

The SAGAIE database is a useful tool to study the turbulent equatorial ionosphere in West-ern and Central Africa, a region of the world where the scintillation phenomenon has not been as well characterized as in South America or South-East Asia ([Morales *et al.*, 2017],[Ji *et al.*, 2015] among other), although it appears to have specificities.

After presenting the SAGAIE network and the context in which the SAGAIE database was collected, the impact of the ionospheric scintillation on the GNSS signal’s amplitude characterized through the S_4 index has been studied in details.

The temporal variability of this index indicates a scintillation apparition cycle depending on the hour of day, and the day of year. Those observations are similar to what was observed in the literature in South-Asia or South-America: scintillation is mainly present close to equinoxes (especially the spring one), and mainly absent during solstices for the peak of solar cycle 24. Some events are however reckoned close to the winter solstice. In terms of hourly variations, scintillation appears at the end of the afternoon (between 6:30 and 8 pm UTC) and weakens then disappears in the middle of the night (between 11:30 pm and 2 am UTC).

The geographical variability of the medium and strong scintillation draws crests between 5° and 15° north and south of the geomagnetic equator, typical of the equatorial phenomena, especially in terms of plasma dynamic. It has moreover been shown that low elevation, although it is naturally a factor of S_4 increase, is not sufficient to observe strong scintillations ; they can only be physically explained through the process giving birth to the equatorial crests.

Finally, the impact of solar activity was observed on the scintillation. SAGAIE covers the peak and the decreasing part of a weak solar cycle: the scintillation strength as well as its occurrence probability may increase in the case of a strong solar cycle observation.

The objective of this work was to make a stenography of ionosphere turbulence in the sub-Saharan zone and to assess whether the scintillation phenomenon could be a blocking point to the development of A-SBAS. Experimental results had indicated this is not the case. Following this, between 2019 and 2021, ASECNA managed the definition and preliminary design phase of its program, awarded to Thales Alenia Space. This phase addressed technical and technological feasibility issues including related to System Architecture, System Performances, RAMS, IVV, Safety, deployment, operation and maintenance topics. On this occasion, the engineering team of Thales Alenia Space have developed an Equatorial Navigation Kernel (NACA solution) that provides satisfying performances. These performances have been validated on the field since 2020 using a real-time demonstrator broadcasting in Western Africa an SBAS augmentation signal compliant with the ICAO SARPs and RTCA MOPS standard.

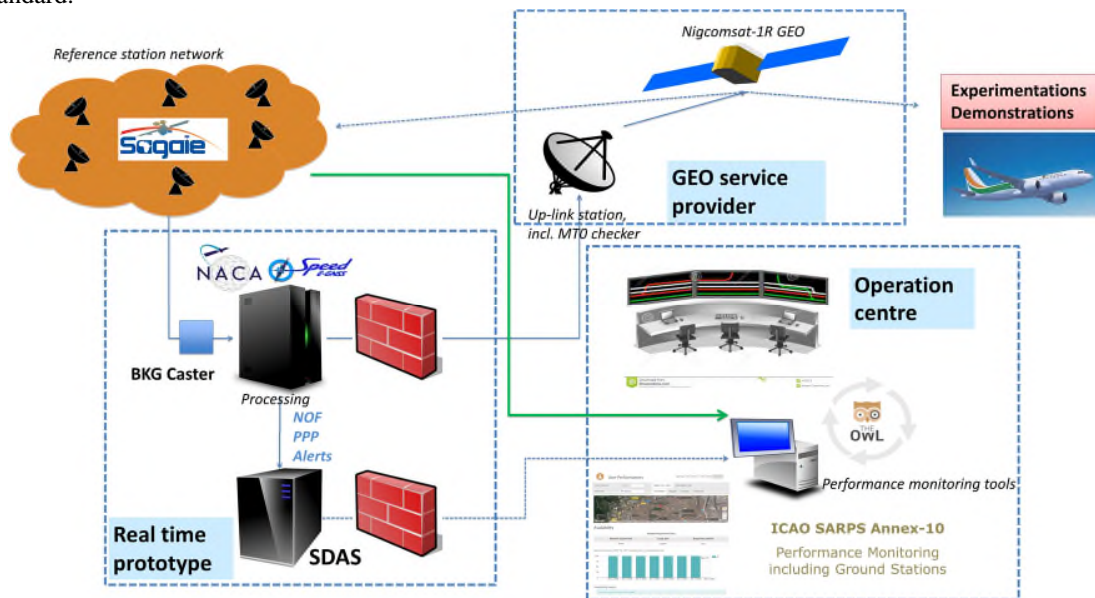


Figure 15 - Pre-operational service architecture

This demonstrator, whose architecture is illustrated in Figure 15, collects GNSS data through a set of stations in Western and Central Africa encompassing the SAGAIE and MONITOR network, augmented by some other stations coming from the

Ionospheric scintillation in West Africa

REGINA network, and feeds the navigation kernel that processes in real time conditions. The navigation message is thus sent to an uplink station that broadcasts the signal to the Nigcomsat 1-R payload, the Nigerian GEO telecommunication satellite. System performances are continuously monitored using TheOwl GNSS monitoring service developed by PildoLabs. In January 2021, several demonstration flights have been conducted by ASECNA at Lome airport (Togo) to showcase the performance of the real time A-SBAS signal to perform SBAS precision approaches and landing procedures. These demonstration flights have proven the efficiency of the A-SBAS augmentation message and its great added-value for air navigation, in particular for approaches to main and secondary African airports that are not served by conventional Instrument Landing System (ILS).

To illustrate these performances the following table provides the worst user pseudorange projected error (SREW) during the 4 days of experimentations. The SREW contains the unmodeled satellite and clock error of the augmented navigation message.

Table 2: SREW values quantiles during the ASECNA aviation demonstration

Day	Mean SREW	SREW@95%	SREW@99%
27/01/2021	0,34m	0,75m	1,04m
28/01/2021	0,32m	0,77m	1,06m
29/01/2021	0,34m	0,79m	1,63m
30/01/2021	0,37m	0,8m	1,09m

In comparison to EGNOS, over the same period, the performance provided by the ASECNA aviation demonstration are very satisfying.

Table 3: Comparison of ASECNA aviation demonstration with respect to EGNOS performance figures

	Mean SREW	SREW@95%	SREW@99%
demo ASECNA	0,34m	0,78m	1,21m
EGNOS	0,82m	1,31m	1,65m

Beside these activities, Thales Alenia Space has developed a new Navigation Kernel compliant to dual-frequency multi-constellation (DFMC) standard messages. Based on these new algorithms, whose performance in fault-free and feared event present a very good behavior in terms of not modeled residual error distribution (see [Authié et al., 2022]), and a proven operational demonstrator capability already available for single frequency SBAS service, Thales Alenia Space has been awarded a contract by the French Space Agency (Centre national d'études spatiales: CNES) to develop a DFMC satellite-based augmentation system (SBAS) prototype with the objective to demonstrate the service in Africa with a L5/E5 augmented signal.

7. ACKNOWLEDGMENTS

The authors would like to thank Damien Serant and Xavier Berenguer from Thales Alenia Space for the help they brought to the data computing. They also thank ASECNA for hosting the SAGAIE stations that produced the raw measurement used in this paper and CNES for having make this particularly valuable GNSS data collection possible.

8. REFERENCES

- [Aarons, 1993] : Aarons, J., 1993, The longitudinal morphology of equatorial F-layer irregularities relevant to their occurrence, Space science reviews, vol.63, issue 3-4, pp 209-243, DOI : 10.1007/BF00750769
- [Authié et al., 2022] : T. Authié, C. Bourga, J. Samson, M. Dall'Orso, 2022, Analysis of the Position and Pseudorange error distributions and autocorrelation functions of a DFMC SBAS, Navitec 2022
- [Blelly & Alcaydé, 2007] : Blelly, P.-L., Alcaydé, D., 2007, Ionosphere, in Kamide, Y., Chian, A., 2007, *Handbook of the Solar-Terrestrial Environment*, Springer-Verlag Berlin Heidelberg, pp. 189-220.

Ionospheric scintillation in West Africa

353

354 [Bhomik & Nandy, 2018] : Bhomik, P., Nandy, D., 2018, Prediction of the strength and timing of sunspot cycle 25 reveal
355 decadal-scale space environmental conditions, *Nat Commun* 9, 5209 (2018), DOI : 10.1038/s41467-018-07690-0.

356

357 [Foucault et al., 2018] : Foucault, E, Blelly, P-L, Marchaudon, A., Serant, D., Trilles, S., 2018, Equatorial Ionosphere
358 Characterization for Sub-Saharan Africa SBAS, *31st ION GNSS+ 2018, 24 September 2018 - 28 September 2018, Miami,*
359 *United States* pp.2222-2240. hal-01915098.

360

361 [Fejer et al., 1991] : Fejer, B. G., de Paula, E. R., Gonzalez, S. A., Woodman, R. F., 1991, Average vertical and zonal F region
362 plasma drifts over Jicamarca , *Journal of geophysical research*, vol.96, no A8, pp 13901-13906, DOI : 10.1029/91JA01171

363

364 [Galiègue et al., 2016] : Galiègue, H., L Féral, and V. Fabbro, 2016, Validity of 2-D electromagnetic approaches to estimate
365 log-amplitude and phase variances due to 3-D ionospheric irregularities, *J. Geophys. Res. Space Physics*, 121, DOI :
366 10.1002/2016JA023233

367

368 [Guo et al., 2019] : Guo, K., Aquino, M., Vadakke Veetil, S., 2019, Ionospheric scintillation intensity fading characteristics
369 and GPS receiver tracking performance at low latitudes, *GPS Solutions* (2019) 23:43, DOI : 10.1007/s10291-019-0835-1

370

371 [ITU-R P531-14, 2019] : ITU recommendation, Ionospheric propagation data and prediction methods required for the design
372 of satellite networks and systems, *P series radiowave propagation, August 2019*

373

374 [Ji et al., 2015] : Ji, S., Chen, W., Weng, D., Wang, Z., 2015, Characteristics of equatorial plasma bubble zonal drift velocity
375 and tilt based on Hong Kong GPS CORS network : from 2001 to 2012, *Journal of geophysical research space physics*, vol.
376 120, pp 7021-7029, DOI : 10.1002/2015JA021493-T

377

378 [Klobuchar et al., 1991] : Klobuchar, J. A., Anderson, D. N., Doherty, P. H., 1991, Model studies of the latitudinal extent of
379 the equatorial anomaly during equinoctial conditions, *Radio Science*, vol.26, no4, pp 1025-1047, DOI : 10.1029/91RS00799

380

381 [Moraes et al., 2017] : Moraes, A. O., Costa, E., Abdu, M. A., Rodrigues, F. S., de Paula, E. R., Oliveira, K. and Perrellan, W.
382 J., 2017, The variability of low-latitude ionospheric amplitude and phase scintillation detected by a triple-frequency GPS
383 receiver, *Radio Sci.*, 52, 439–460, DOI : 10.1002/2016RS006165

384

385 [Mushini, 2012] : Mushini, S. C., 2012, Characteristics of scintillating GPS signals at high latitudes during solar minima, PhD
386 thesis from University of New Brunswick

387

388 [Rama Rao et al., 2006] : Rama Rao P. V. S., Gopi Krishna S., Niranjana, K., Prasad, D. S. V. V. D., 2006. Study of spatial and
389 temporal characteristics of L-band scintillations over the Indian low-latitude region and their possible effects on GPS
390 navigation, *Annales Geophysicae, European Geosciences Union, 2006, 24 (6), pp.1567-1580*, DOI : 10.5194/angeo-24-1567-
391 2006

392

393 [Rino, 1979] : Rino, C. L., 1979, A power law phase screen model of ionospheric scintillation, 1. Weak scatter, *Radio Science*,
394 vol. 14, n°6, pp. 1135-1143, DOI : 10.1029/RS014i006p01135

395

396 [Rishbeth, 1997] : Rishbeth, H., 1997, The ionospheric E-layer and F-layer dynamos – a tutorial review, *Journal of*
397 *Atmos and Solar-terrestrial physics*, vol.59, no 15, pp 1873-1880, DOI : 10.1016/S1364-6826(97)00005-9

398

399 [Secretan et al., 2014] : Secretan, H., Rougerie, S., Ries, L., Monnerat, M., Giraud, J., Kamení, R., 2014, SAGAIE a GNSS
400 network for investigating ionospheric behavior in sub-saharan regions, *InsideGNSS* pp 46-58, issue september/october 2014.

401

402 [Van Dierendonck et al., 1993] : Van Dierendonck, A. J., Klobuchar, J., Quyen, H., 1993, Ionospheric Scintillation Monitoring
403 Using Commercial Single Frequency C/A Code Receivers, *Proceedings of the 6th International Technical Meeting of the*
404 *Satellite Division of The Institute of Navigation (ION GPS 1993), Salt Lake City, UT, pp. 1333-1342.*